FIBROSIS

NUAK1 promotes organ fibrosis via YAP and TGF-β/SMAD signaling

Tianzhou Zhang[1], Xiaolin He[1], Lauren Caldwell[2], Santosh Kumar Goru[1], Luisa Ulloa Severino[1], Monica F. Tolosa[1], Paraish S. Misra[1], Caitríona M. McEvoy[1], Tania Christova[3], Yong Liu[4], Cassandra Atin[1], Johnny Zhang[1], Catherine Hu[1], Noah Vukosa[1], Xiaolan Chen[1], Adriana Krizova[5], Anish Kirpalani[6], Alex Gregorieff[2]†, Ruoyu Ni[2], Kin Chan[2], Mandeep K. Gill[3], Liliana Attisano[3], Jeffrey L. Wrana[2], Darren A. Yuen[1]*

Fibrosis is a central pathway that drives progression of multiple chronic diseases, yet few safe and effective clinical antifibrotic therapies exist. In most fibrotic disorders, transforming growth factor–β (TGF-β)–driven scarring is an important pathologic feature and a key contributor to disease progression. Yes-associated protein (YAP) and transcriptional coactivator with PDZ-binding motif (TAZ) are two closely related transcription cofactors that are important for coordinating fibrogenesis after organ injury, but how they are activated in response to tissue injury has, so far, remained unclear. Here, we describe NUAK family kinase 1 (NUAK1) as a TGF-β–inducible profibrotic kinase that is up-regulated in multiple fibrotic organs in mice and humans. Mechanistically, we show that TGF-β induces a rapid increase in NUAK1 in fibroblasts. NUAK1, in turn, can promote profibrotic YAP and TGF-β/SMAD signaling, ultimately leading to organ scarring. Moreover, activated YAP and TAZ can induce further NUAK1 expression, creating a profibrotic positive feedback loop that enables persistent fibrosis. Using mouse models of kidney, lung, and liver fibrosis, we demonstrate that this fibrogenic signaling loop can be interrupted via fibroblast-specific loss of NUAK1 expression, leading to marked attenuation of fibrosis. Pharmacologic NUAK1 inhibition also reduced scarring, either when initiated immediately after injury or when initiated after fibrosis was already established. Together, our data suggest that NUAK1 plays a critical, previously unrecognized role in fibrogenesis and represents an attractive target for strategies that aim to slow fibrotic disease progression.

INTRODUCTION

Chronic fibrotic disorders are responsible for nearly half of all deaths in the developed world (*1*). Thought to represent a pathologic wound healing response to persistent injury, fibrosis is a common feature of chronic diseases affecting nearly every tissue in the body (*2*). Studies of different organs have revealed a remarkable similarity in the profibrotic signaling cascades that drive the scarring process, suggesting that the many different insults that incite organ injury may result in activation of a common fibrogenic pathway of chronic disease. Despite this emerging theme, efforts to develop safe and effective clinical antifibrotic therapies have been largely unsuccessful to date. Nowhere is this truer than in the kidney, where fibrosis is a self-perpetuating damage pathway activated by nearly all forms of chronic kidney disease, and yet, no renal-specific antifibrotic therapies have been developed to date (*3*, *4*).

Transforming growth factor–β (TGF-β) is an important driver of fibrosis in the kidney and other organs (*5*–*7*). We (*8*) and others (*9*–*13*) recently demonstrated that fibroblast responsiveness to TGF-β is dependent on the downstream effectors of the Hippo pathway, the transcription cofactors Yes-associated protein (YAP) and transcriptional coactivator with PDZ-binding motif (TAZ) [also known as WW domain-containing transcription regulator 1 (WWTR1)]. The activity of YAP and TAZ is regulated primarily by their subcellular localization. In healthy tissues, YAP and TAZ localize mostly in the fibroblast cytosol, where they are inactive. In contrast, YAP and TAZ localize preferentially to the fibroblast nucleus in fibrotic tissue (*14*), where they can promote profibrotic signaling through TGF-β–dependent and TGF-β–independent mechanisms (*10*, *12*, *13*, *15*–*19*). Together, these reports have established YAP and TAZ as critical drivers of organ fibrosis, although an important question that remains unanswered has been how these profibrotic transcription cofactors are activated after organ injury.

In a search for previously unidentified regulators of fibrogenesis, we transcriptionally profiled archival human kidney biopsy specimens with varying degrees of fibrosis using RNA sequencing (RNA-seq). Our analysis identified the AMPK (5' adenosine monophosphate-activated protein kinase)–related kinase *NUAK1* [also known as AMPK-related protein kinase 5 (*ARK5*)] as a gene that is strongly associated with fibrosis, TGF-β signaling, and poor outcomes in human chronic kidney disease. Corresponding mouse studies demonstrated that NUAK1 expression is increased not only in the damaged kidney but also in many fibrotic tissues. Using genetic and pharmacologic tools, we further show that NUAK1 is a critical and previously unrecognized TGF-β–induced activator of YAP in fibroblasts, working in concert with TGF-β/SMAD signaling to promote fibrogenesis in multiple organs. We also show that YAP and TAZ drive expression of NUAK1 to create a profibrotic positive feedback loop that

[1]Keenan Research Centre for Biomedical Science, Li Ka Shing Knowledge Institute, St. Michael's Hospital (Unity Health Toronto) and Department of Medicine, University of Toronto, Toronto, Ontario M5B 1T8, Canada. [2]Center for Systems Biology, Lunenfeld-Tanenbaum Research Institute, Mt. Sinai Hospital and Department of Molecular Genetics, University of Toronto, Toronto, Ontario M5G 1X5, Canada. [3]Donnelly Centre and Department of Biochemistry, University of Toronto, Toronto, Ontario M5S 1A8, Canada. [4]Ontario Institute of Cancer Research, Toronto, Ontario M5G OA3, Canada. [5]Department of Laboratory Medicine and Pathobiology, School of Graduate Studies, University of Toronto, Toronto, Ontario M5S 1A8, Canada. [6]Department of Medical Imaging, St. Michael's Hospital (Unity Health Toronto) and University of Toronto, Toronto, Ontario M5B 1W8, Canada.
*Corresponding author. Email: darren.yuen@utoronto.ca
†Present address: Department of Pathology, McGill University and Research Institute of the McGill University Health Center, Montreal, Quebec H4A 3J1, Canada.

can perpetuate fibrosis. NUAK1 deletion and/or inhibition attenuated this positive feedback signaling and protected against injury-induced fibroblast activation and downstream fibrosis.

RESULTS

Profiling the transcriptome in human transplant kidneys

To gain insights into the pathogenesis of human kidney fibrosis, we examined the transcriptomes of 18 archival transplant kidney biopsy samples from patients in whom interstitial fibrosis was graded using a standardized histology classification system (Banff criteria) (*20*) and for whom renal function [as measured by estimated glomerular filtration rate (eGFR)] was subsequently tracked over a maximum of 4 years (Fig. 1A and table S1). Using this dataset, we considered whether correlation of gene expression with histopathology and/or future changes in kidney function might identify genes specifically associated with poor clinical outcome.

Comparison of future kidney function with either initial fibrotic score or starting eGFR function showed correlations that were generally weak (Fig. 1A). However, when we assessed whether transcriptional changes might be associated with these alterations, we observed gene expression correlations with both fibrosis and the slope of kidney function change after biopsy (table S2). Furthermore, plotting the correlation coefficients for each transcript in a two-dimensional matrix revealed a clear association with fibrosis and kidney function, with two main clusters of genes identified ($P < 0.02$ by permutation; Fig. 1B). The first cluster was composed of putative disease drivers (pDDs) whose expression correlated positively with high fibrosis score and negatively with future kidney function (red dashed box, 225 genes; Fig. 1B). In contrast, the second cluster, composed of putative disease suppressors, was defined by genes that associated with low fibrotic burden (negative correlation with fibrosis score) and correlated positively with future kidney function (blue dashed box, 65 genes; Fig. 1B). Functional annotation showed that poor disease outcome was dominated by genes encoding components of signaling pathways and proteins involved in extracellular matrix (ECM) remodeling [number of genes assigned to "signaling" + "ECM" + "proteases" (116) divided by the total number of pDD genes (225) = 52%; table S2]. In contrast, good disease outcome was dominated by genes encoding enzymes involved in cell metabolism (25 of 65; 38%).

Analysis of pathways in pDD showed ECM components that included collagens, the proteoglycans lumican and versican, and CSGALNACT1, a key enzyme in chondroitin chain biosynthesis, as well as proteases (Fig. 1C and table S2). In the latter group, the prolyl endopeptidase fibroblast-activating protein was notable, as it has been linked to fibrosis and tissue remodeling (*21*). Similarly, we identified three tyrosine kinase receptors, *PDGFRA*, *PDGFRB*, and *DDR2*, which are strongly implicated in human fibrotic diseases (Fig. 1C and table S2) (*22*–*24*). Profibrotic transcription factors including *ZEB2* (*25*) and *HIF1A* (*26*) were also identified. Last, key morphogen signaling pathways were also evident, particularly WNT signaling components such as DKK3, which drives activation of cancer-associated fibroblasts (*27*) and TGF-β family ligands. The latter included *TGFB2* and Activin A (*INHBA*), whereas *TGFB3* displayed slightly less association with poor outcome (Fig. 1D), and neither *TGFB1* nor *INHBB* was associated with any outcome. In summary, transcriptional profiling of human transplant kidneys defines transcriptional changes associated with disease outcome and identifies known drivers of fibrotic disease.

NUAK1 expression is a pDD that is up-regulated in fibrotic mouse tissue

TGF-β has long been recognized as a key driver of fibrotic disease that leads to loss of organ function. Because TGF-β–induced cellular responses are highly contextual, we used a set of carefully annotated fibroblast-associated TGF-β target genes (*28*) to perform single-sample Gene Set Enrichment Analysis (ssGSEA) on our transplant kidney tissue. Correlation of fibroblast–TGF-β ssGSEA scores with pDDs showed a significant association ($P < 0.01$) with 51 genes, including *DKK3*, *PDGFRA*, *PDGFRB*, and *DDR2* (table S3). Another signaling component that we noted in this group was NUAK1 (Fig. 1D), an AMPK family serine/threonine kinase recently reported to be induced by TGF-β (*29*) but otherwise not previously associated with fibrosis. Analysis of *NUAK1* showed that its expression was strongly correlated with the fibroblast–TGF-β signature (Fig. 1E).

Given our finding of correlations between *NUAK1* expression, poor kidney outcomes, high fibrosis scores, and this fibroblast–TGF-β signature, we next examined the functional relevance of NUAK1 in fibrosis. For this, we first assessed *Nuak1* expression in mouse models of kidney, lung, and liver fibrosis. *Nuak1* expression was low in healthy mouse kidneys (fig. S1), whereas *Nuak1* mRNA and NUAK1 protein increased markedly after unilateral ureteral obstruction (UUO)–induced fibrotic injury, a well-established model of TGF-β–driven kidney fibrosis (fig. S1, A to C). Costaining for *Nuak1* mRNA and α–smooth muscle actin (α-SMA) protein, which identifies activated renal myofibroblasts, demonstrated that increased *Nuak1* expression was mostly associated with interstitial myofibroblasts, cells identified by their expression of α-SMA (fig. S1, C and D). Similarly, analysis of *Nuak1* expression in lung and liver fibrosis models showed increased *Nuak1* expression in fibrotic organs (fig. S2). Together, our data show that *Nuak1* expression is increased in fibrotic tissues and is associated with declining function in human transplant kidneys.

NUAK1 expression is regulated by TGF-β, YAP, and TAZ

Our observation that NUAK1 expression is up-regulated in multiple fibrotic tissues and is correlated with a fibroblast–TGF-β gene signature in human kidneys suggested that NUAK1 expression may be TGF-β inducible. Using cultured renal fibroblasts, we found that NUAK1 was induced by TGF-β (fig. S3), as previously reported in epithelial cells, myoblasts, and skin fibroblasts (*29*). As we previously showed that TGF-β/SMAD and YAP/TAZ signaling pathways intersect to drive fibrotic responses (*8*), we next examined *Nuak1* expression upon *Yap* and/or *Taz* or *Smad2/3* silencing. Silencing of either *Yap* or *Taz* alone reduced basal *Nuak1* mRNA amounts modestly, whereas silencing both together had an additive effect (Fig. 2, A to C). Likewise, SMAD2/3 deficiency reduced *Nuak1* mRNA quantity (fig. S4). Furthermore, when we overexpressed constitutively active YAP (YAP5SA) and TAZ (TAZ4SA) in fibroblasts, we noted increases in NUAK1 protein (Fig. 2D) and *Nuak1* mRNA (Fig. 2E). These results are consistent with the identification of *NUAK1* in a systematic screen for YAP/TAZ target genes identified by profiling genome occupancy (*30*). Together, these data suggest that NUAK1 expression is regulated not only by TGF-β/SMAD signaling but also by both YAP and TAZ.

To confirm the in vivo relevance of our findings, we generated tamoxifen-inducible, fibroblast-specific YAP/TAZ-deficient mice (Col1a2-Cre/ERT$^{+/-}$ and *Yap*/*Taz*$^{fl/fl}$ mice) (*31*, *32*) and subjected them to UUO-induced fibrotic injury, followed by tamoxifen

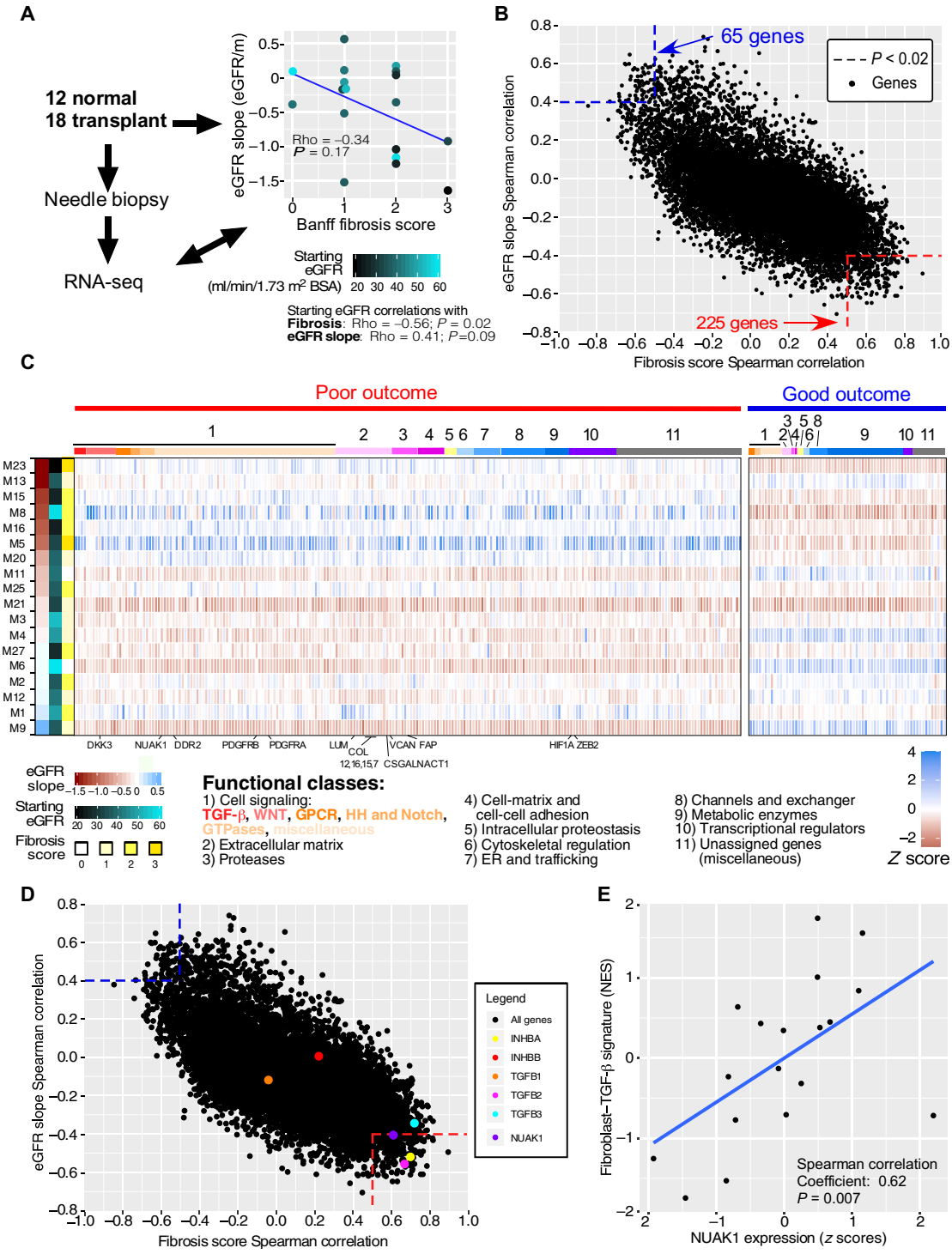

Fig. 1. NUAK1 is a putative YAP/TAZ-regulated gene whose expression correlates with human kidney fibrotic burden and loss of renal function. (**A**) Study design. Eighteen human kidney transplant biopsies were assessed for interstitial fibrosis according to the standardized Banff classification system (*20*) and compared with starting estimated glomerular filtration rates (eGFRs; milliliters per minute per 1.73 m^2 body surface area) and future kidney function (eGFR slope, milliliters per minute per 1.73 m^2 body surface area per month) as indicated. RNA-seq was also performed on RNA isolated from these biopsy tissues, and biopsies were obtained from 12 prospective living kidney donors with normal renal function and no pathologic abnormalities. (**B**) Correlations of gene expression with outcome. For the ~13,500 protein-coding transcripts identified across all 18 transplant biopsies, Spearman correlation coefficients were calculated for the relationships between gene expression and fibrosis score (*x* axis) and gene expression and slope of eGFR change after biopsy (*y* axis) and plotted in a two-dimensional matrix. Each black dot represents a unique transcript, and regions with $P < 0.02$ (by permutation) are marked. (**C**) Expression of genes associated with outcome. The expression in transplant kidneys of genes found in the two quadrants identified in (B) is plotted as a *z*-score heatmap (scale). On the left, each study participant is identified by their study identifier (M#). Functional clusters are indicated, as are the pathological and clinical parameters for each patient. (**D**) Correlation of TGF-β family members with fibrosis and outcome. The positions of the indicated TGF-β family members and NUAK1 on the correlation plot are marked as indicated. (**E**) Correlation of NUAK1 expression with a fibroblast–TGF-β gene signature. Single-sample Gene Set Enrichment Analysis (ssGSEA) was performed for a fibroblast–TGF-β target gene set and compared with NUAK1 expression. BSA, body surface area; ER, endoplasmic reticulum; GPCR, G protein–coupled receptor; HH, Hedgehog; LUM, lumican; m, month; NES, normalized enrichment score; VCAN, versican; GTPases, guanosine triphosphatases.

administration to induce *Yap* and *Taz* deletion. In situ hybridization confirmed that loss of YAP and TAZ strongly reduced the amount of *Nuak1* mRNA in α-SMA^+ myofibroblasts (Fig. 2, F and G). Our findings therefore suggest that TGF-β, YAP, and TAZ are important promoters of fibroblast *Nuak1* expression, both basally and in the setting of fibrotic injury.

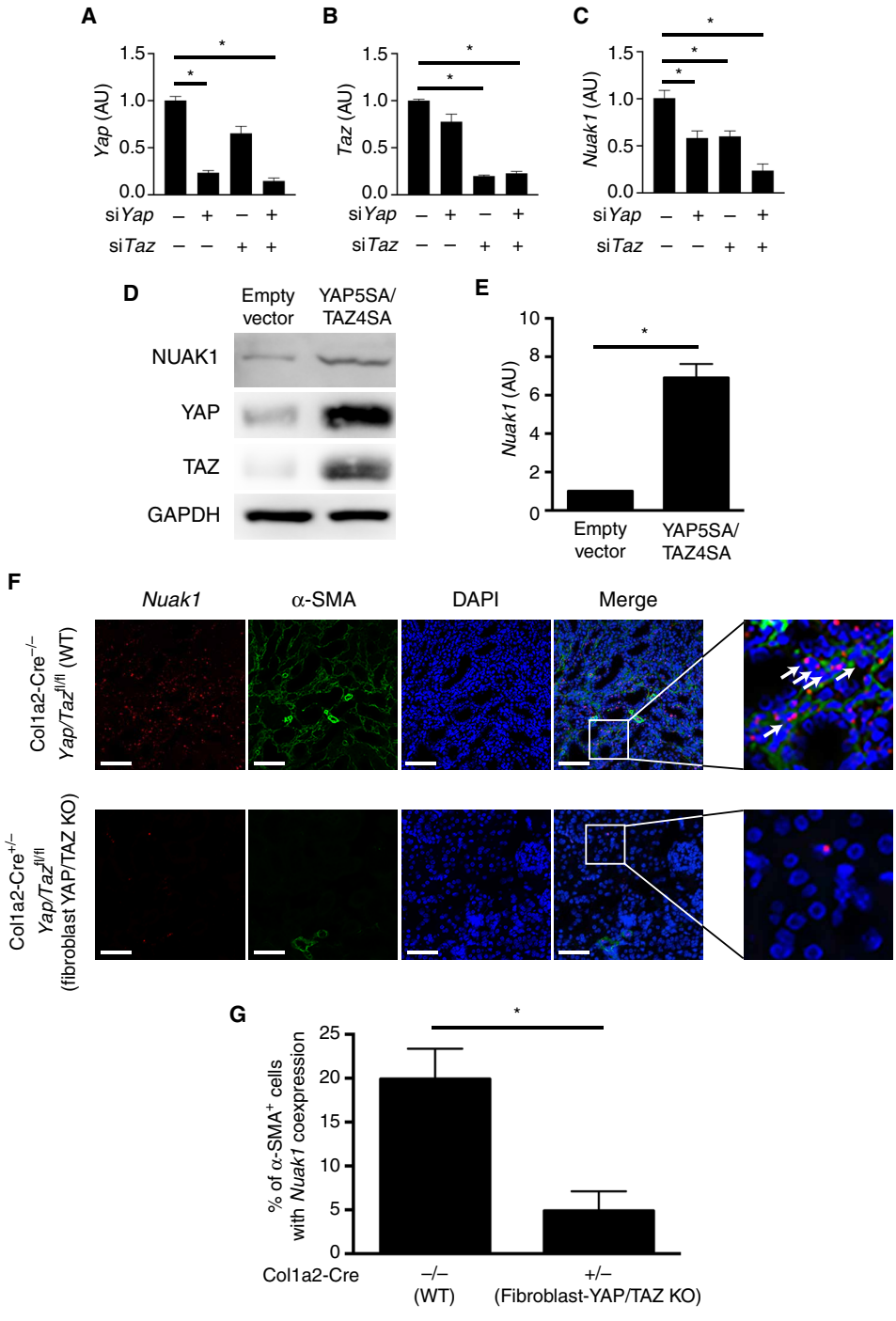

Fig. 2. YAP and TAZ promote NUAK1 expression in renal fibroblasts in vitro and in vivo. NRK49F rat renal fibroblasts were cultured on gelatin-coated 2-kPa silicone gels. (**A** to **C**) YAP and/or TAZ were silenced, and the amounts of *Yap*, *Taz*, and *Nuak1* mRNA were examined ($n = 3$ per condition). (**D** and **E**) Constitutively active YAP (YAP5SA) and TAZ (TAZ4SA) or an empty vector were ectopically expressed in NRK49F fibroblasts, and the amounts of both (D) NUAK1 protein and (E) *Nuak1* mRNA were examined ($n = 3$ per condition). (**F** and **G**) To examine whether YAP and TAZ regulate *Nuak1* expression in renal fibroblasts in vivo, we generated fibroblast-specific YAP/TAZ-deficient mice (Col1a2-Cre$^{+/-}$/ERT *Yap/Taz*$^{fl/fl}$). Mice were subjected to left-sided UUO ($n = 4$ per group), and tamoxifen was administered between days 0 and 6 after surgery to activate expressed Cre recombinase. Obstructed kidneys were harvested 7 days after surgery. White arrows indicate dual-positive α–smooth muscle actin–positive (α-SMA$^+$) *Nuak1*$^+$ fibroblasts. Scale bars, 50 μm. One-way ANOVA with post hoc Fisher's least significant difference and Student's *t* test was used for comparisons. Quantitative data are presented as means ± SEM. *$P < 0.05$. AU, arbitrary units; si*Yap*, Yap-targeting siRNA; si*Taz*, Taz-targeting siRNA; KO, knockout; WT, wild type. DAPI, 4′,6-diamidino-2-phenylindole.

NUAK1 mediates TGF-β– and YAP-associated fibroblast activation

Both YAP/TAZ and TGF-β are critical regulators of fibrosis in many different tissues, and growing evidence suggests that TGF-β signaling is closely linked with YAP and TAZ activity (*8*, *10*, *11*, *15*, *16*, *33*). Our finding that fibroblast NUAK1 is a YAP/TAZ- and TGF-β–regulated kinase whose expression is increased in fibrotic tissues suggested that NUAK1 might serve as a critical, previously unrecognized link between these two profibrotic pathways. To explore this, we used a previously developed gel-based cell culture system that mimics the soft matrix environment of epithelial-rich tissues such as the kidney (*8*). Under these conditions, YAP and TAZ are preferentially localized to the cytoplasm, mimicking cells in the healthy kidney (*8*). In contrast, in cells cultured on artificially stiff surfaces, such as tissue culture plastic, YAP and TAZ are found preferentially in the nucleus, a phenotype that does not replicate the healthy in vivo setting (*12*, *14*). Using this gel-based culture system, we first examined the effects of TGF-β stimulation on the activity of YAP and TAZ in fibroblasts. TGF-β stimulation led to dephosphorylation of the S127 residue of YAP, a key step in YAP activation (Fig. 3A). In contrast, TAZ phosphorylation was largely unaffected, suggesting that TGF-β primarily activates YAP in fibroblasts (Fig. 3, A and B, and fig. S3). TGF-β–induced YAP dephosphorylation was associated with YAP nuclear accumulation (Fig. 3C) and increased transcription of *Ankrd1*, *Ccn2*, and *Ccn1* (Fig. 3, D to F). Because these genes are also regulated by SMADs (*34*–*36*), we next overexpressed activated YAP (YAP5SA) in NRK49F fibroblasts in the presence or absence of a TGF-β/SMAD signaling inhibitor, finding that YAP5SA increased the expression of these genes, even in the absence of basal SMAD signaling (fig. S5). We also tested the effects of TGF-β on the activity of a TEA domain (TEAD) element–driven luciferase reporter plasmid (*37*) that reflects YAP/TEAD transcriptional activity. As expected, TGF-β increased TEAD element–driven luciferase reporter activity (Fig. 3G). TGF-β stimulation also increased the expression of fibrosis-associated genes encoding α-SMA (*Acta2*) and collagens (*Col1a1*,

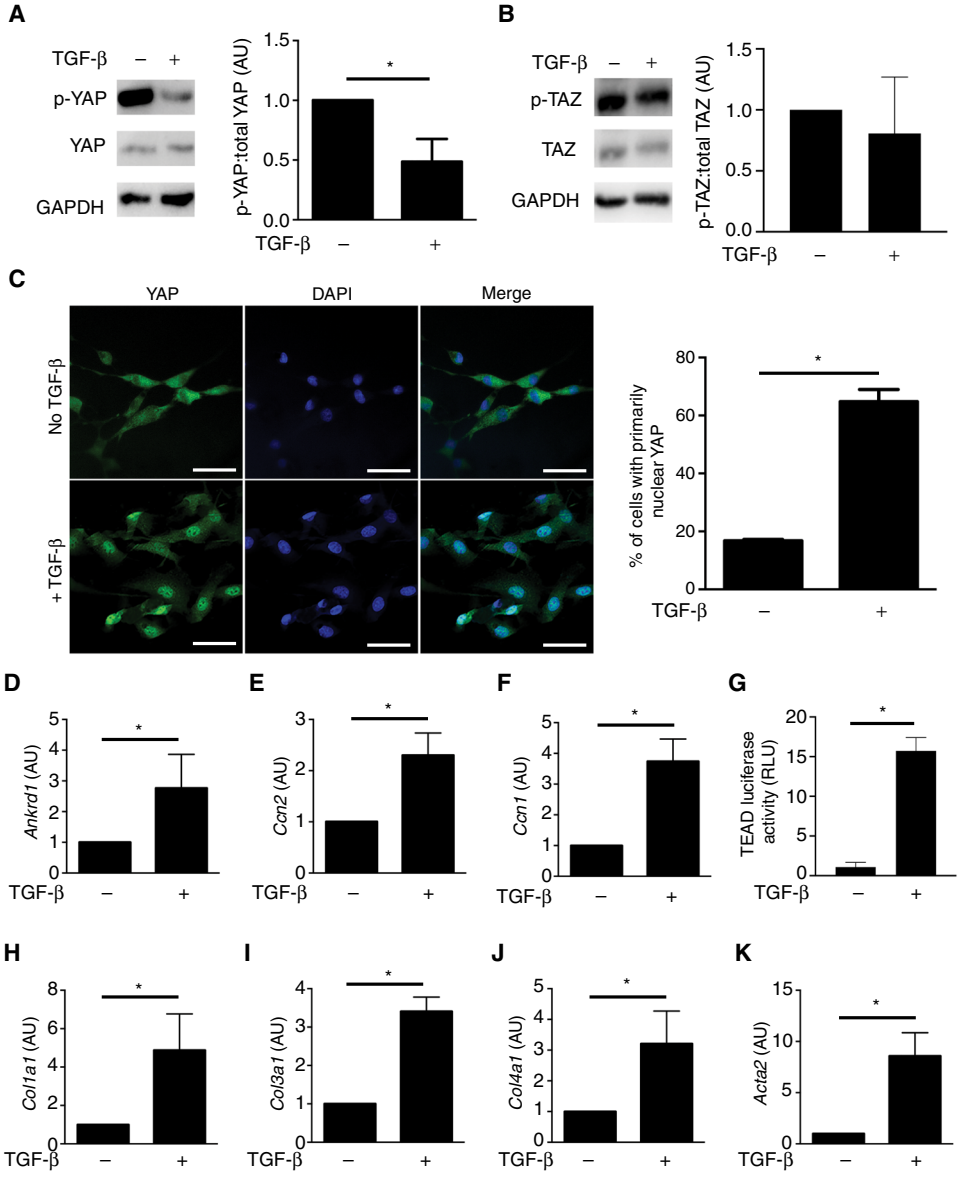

Fig. 3. TGF-β stimulation leads to YAP activation and the expression of fibrosis-associated genes in fibroblasts. NRK49F fibroblasts were cultured on gelatin-coated 2-kPa silicone gels and stimulated with TGF-β (5 ng/ml). The effect of TGF-β on YAP and TAZ activity was documented by assessing (**A**) YAP S127 and (**B**) TAZ S89 phosphorylation (after 4 hours of TGF-β stimulation; $n = 3$ per condition), (**C**) YAP nuclear localization (after 4 hours of TGF-β stimulation; $n = 3$ per condition), and the expression of (**D**) *Ankrd1*, (**E**) *Ccn2*, and (**F**) *Ccn1* or (**G**) TEAD luciferase reporter activity as a readout of YAP transcriptional activity (after 16 hours of TGF-β stimulation; $n = 3$ per condition). Similarly, the effect of 16-hour TGF-β stimulation on the expression of the following fibrosis-associated genes was also assessed ($n = 3$ per condition): (**H**) *Col1a1*, (**I**) *Col3a1*, (**J**) *Col4a1*, and (**K**) *Acta2*. Transcript amounts were normalized to the housekeeper *Gapdh*. Student's *t* test was used for comparisons. Quantitative data are presented as means ± SEM. *$P < 0.05$. Scale bars, 20 μm. p-YAP, phospho-S127 YAP. p-TAZ, phospho-S89 TAZ; RLU, relative light units.

Col3a1, and *Col4a1*) (Fig. 3, H to K). Activated YAP alone also increased the expression of these fibrosis-associated genes, but unlike for *Ankrd1*, *Ccn2*, and *Ccn1*, this effect was largely blocked by inhibition of basal SMAD signaling (fig. S5). These data indicate that TGF-β promotes YAP activation and that YAP contributes to the multiple profibrotic effects of TGF-β/SMAD signaling.

Because TGF-β induces a rapid increase in the amount of fibroblast NUAK1 protein (fig. S3), we next asked whether NUAK1 might mediate TGF-β–induced YAP activation. For this, we treated NRK49F fibroblasts with HTH-02-006, a NUAK inhibitor (*38*). Our experiments suggested that NUAK inhibition decreases TGF-β–induced YAP activation, as evidenced by a trend toward less YAP dephosphorylation (a marker of activated YAP; Fig. 4A), and a smaller reduction in inactive, cytoplasmic YAP (gray bars, Fig. 4B), when cells were stimulated with TGF-β in the presence of HTH-02-006. We also noted diminished TGF-β–induced TEAD element–driven luciferase reporter activity and reduced expression of *Ankrd1*, *Ccn2*, and *Ccn1* when HTH-02-006 was coadministered (Fig. 4, C to E, and fig. S6). NUAK inhibition with HTH-02-006 also reduced basal and TGF-β–induced expression of fibrosis-associated genes (Fig. 4, F to H). Inhibition with another NUAK inhibitor, WZ4003 (*39*), also decreased TGF-β–induced YAP nuclear accumulation, TEAD element–driven luciferase reporter activity, and the expression of *Ankrd1*, *Ccn2*, *Ccn1*, and various fibrosis-associated genes (fig. S6). NUAK inhibition with either HTH-02-006 or WZ4003 similarly diminished TGF-β–induced expression of these genes in human lung fibroblasts (fig. S7). To confirm these results, we next silenced *Nuak1* in NRK49F rat fibroblasts using small interfering RNAs (siRNAs). *Nuak1* knockdown had similar effects as either HTH-02-006 or WZ4003, reducing TGF-β–induced YAP nuclear localization (fig. S8). It also attenuated the ability of TGF-β to induce the expression of *Ankrd1*, *Ccn2*, *Ccn1*, *Col1a1*, *Col3a1*, and *Acta2* (Fig. 4, I to N) without affecting fibroblast apoptosis rates ($P = 0.11$; fig. S9). As further confirmation, we showed that the expression of *Ankrd1*, *Ccn2*, *Ccn1*, and fibrosis-associated genes was rescued by cotransfecting wild-type human *NUAK1* but not a kinase-dead (K84M) *NUAK1* mutant (Fig. 4, I to N).

In the above experiments, we demonstrated that in fibroblasts, TGF-β–induced expression of *Ankrd1*, *Ccn2*, *Ccn1*, and fibrosis-associated genes requires NUAK1 kinase activity. We next asked whether NUAK1 is sufficient to drive YAP activation on its own by overexpressing wild-type NUAK1 in NRK49F fibroblasts. As shown in fig. S10A, NUAK1 overexpression appeared to reduce YAP S127

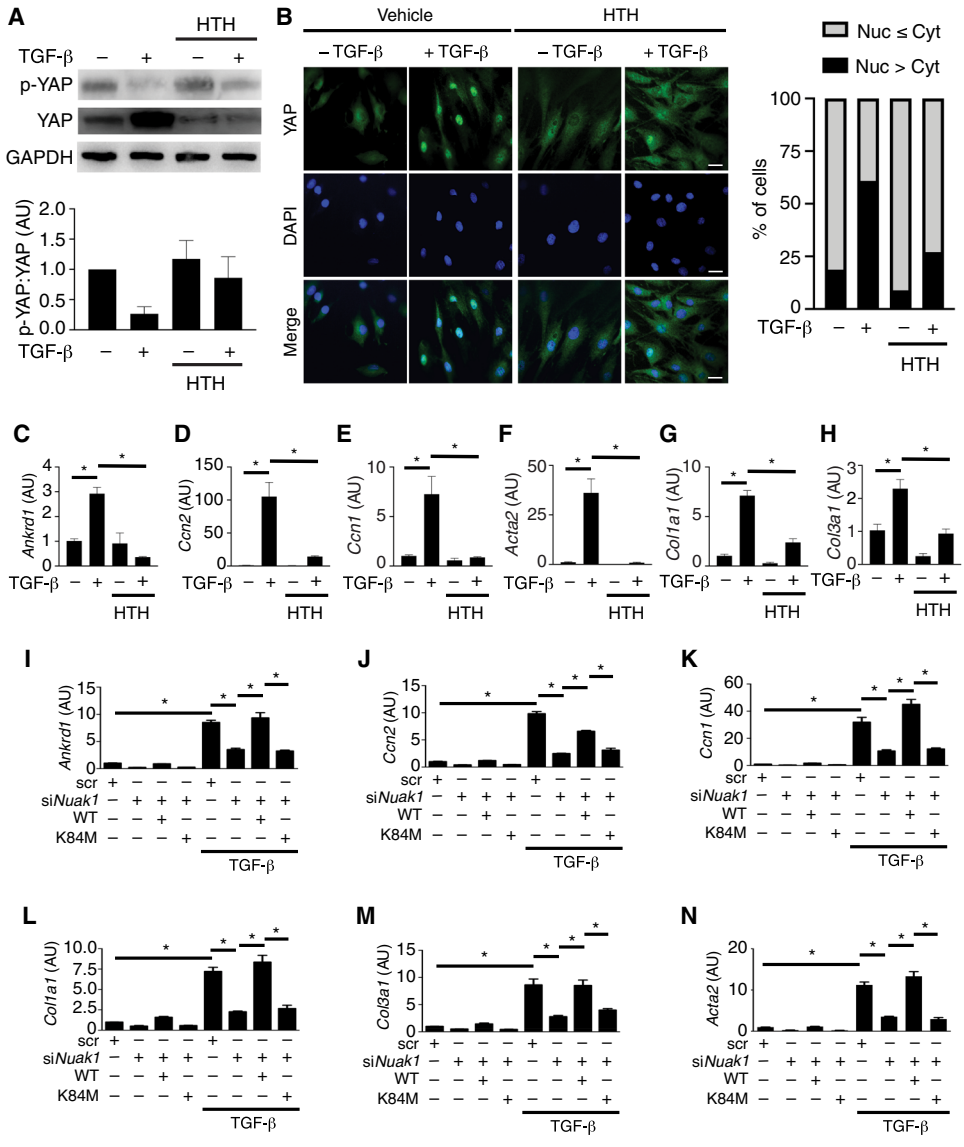

Fig. 4. NUAK1 mediates the TGF-β–induced expression of profibrotic genes in fibroblasts. NRK49F fibroblasts were cultured on gelatin-coated 2-kPa silicone gels and stimulated with or without TGF-β (5 ng/ml). The NUAK inhibitor HTH-02-006 (HTH; 100 nM) was used to assess the effects of NUAK1 inhibition in NRK49F fibroblasts on (**A**) YAP S127 phosphorylation ($n = 5$ per condition); (**B**) YAP nuclear localization ($n = 5$ to 6 per condition); (**C** to **E**) the expression of (C) *Ankrd1*, (D) *Ccn2*, and (E) *Ccn1*; and (**F** to **H**) the expression of the fibrosis-associated genes (F) *Acta2*, (G) *Col1a1*, and (H) *Col3a1*. For (A) and (B), cells were treated with or without TGF-β and HTH-02-006 for 4 hours. Scale bars, 20 μm. For (C) to (H), cells were treated with TGF-β and HTH-02-006 for 16 hours. The expression of endogenous *Nuak1* was silenced in NRK49F fibroblasts using siRNA (si*Nuak1*) and rescued after ectopic expression of wild-type or kinase-dead (K84M) human NUAK1 ($n = 3$ per condition). Scrambled siRNA (scr) was used as a control. The expression of (**I**) *Ankrd1*, (**J**) *Ccn2*, (**K**), *Ccn1*, (**L**) *Col1a1*, (**M**) *Col3a1*, and (**N**) *Acta2* was then examined after 16-hour stimulation with or without TGF-β. All transcript amounts were normalized to that of *Gapdh*. One-way ANOVA with post hoc Fisher's least significant difference was used for comparisons. Quantitative data are presented as means ± SEM. *$P < 0.05$.

phosphorylation in NRK49F fibroblasts even in the absence of TGF-β/SMAD signaling, whereas kinase-dead NUAK1 (K84M) did not. We next showed that wild-type NUAK1 overexpression increased YAP nuclear localization, even in the presence of a TGF-β receptor kinase inhibitor, suggesting that NUAK1 can activate YAP independently of TGF-β signaling (fig. S10, B and C). Moreover, wild-type NUAK1, but not its kinase-dead variant, increased the expression of *Ankrd1*, *Ccn2*, and *Ccn1* (fig. S10, D to F), as well as various collagens (fig. S10, G and H). Similar to our findings with YAP overexpression, inhibition of TGF-β/SMAD signaling largely blocked NUAK1-induced collagen expression but not the increased expression of *Ankrd1*, *Ccn2*, and *Ccn1* (fig. S10). Last, NUAK1-induced expression of *Ankrd1*, *Ccn2*, *Ccn1*, and various fibrosis-associated genes (collagens and α-SMA) was abrogated by pharmacologic YAP inhibition using verteporfin (fig. S11) (*8*, *10*). Together, our data suggest that NUAK1 is induced by TGF-β, YAP, and TAZ but may also act as a key node mediating cross-talk between profibrotic signaling pathways downstream of TGF-β in fibroblasts.

Fibroblast NUAK1 is a critical regulator of YAP activation in vivo that drives organ fibrosis

Our results suggest that NUAK1 and YAP/TAZ may act in a positive feedback loop to promote fibroblast activation. To better understand the role that fibroblast NUAK1 plays in regulating fibrosis in vivo, we next generated tamoxifen-inducible, fibroblast-specific NUAK1-deficient mice (Col1a2-Cre/ERT$^{+/-}$, mTmG^{+}, and *Nuak1*$^{fl/fl}$ mice; fig. S12). Consistent with our in vitro findings, fibroblast NUAK1 deficiency resulted in a marked attenuation of UUO-induced kidney fibrosis (Fig. 5, A to C). Molecular markers of fibrosis were similarly reduced in the setting of fibroblast NUAK1 deficiency (Fig. 5, D to F). As we and others have shown previously, UUO-induced fibrotic injury also resulted in fibroblast YAP activation, as evidenced by enhanced nuclear YAP localization (fig. S13) (*8*, *40*). Similarly, the expression of *Ankrd1*, *Ccn2*, and *Ccn1*, genes whose expression is regulated partly by YAP, was also increased in UUO animals (Fig. 5, G to I) (*8*, *40*). NUAK1 deficiency reduced this UUO-associated YAP nuclear staining in fibroblasts and diminished expression of *Ankrd1*, *Ccn2*, and *Ccn1* (fig. S13 and Fig. 5, G to I). To further confirm the importance of fibroblast NUAK1 in driving kidney fibrosis, we next subjected fibroblast-specific NUAK1-deficient mice to folic acid–induced nephropathy, a model of crystal-induced renal injury that leads to subsequent fibrosis (*41*). Consistent with our results in the UUO model, fibroblast NUAK1 deficiency reduced folic acid–induced renal fibrosis (fig. S14).

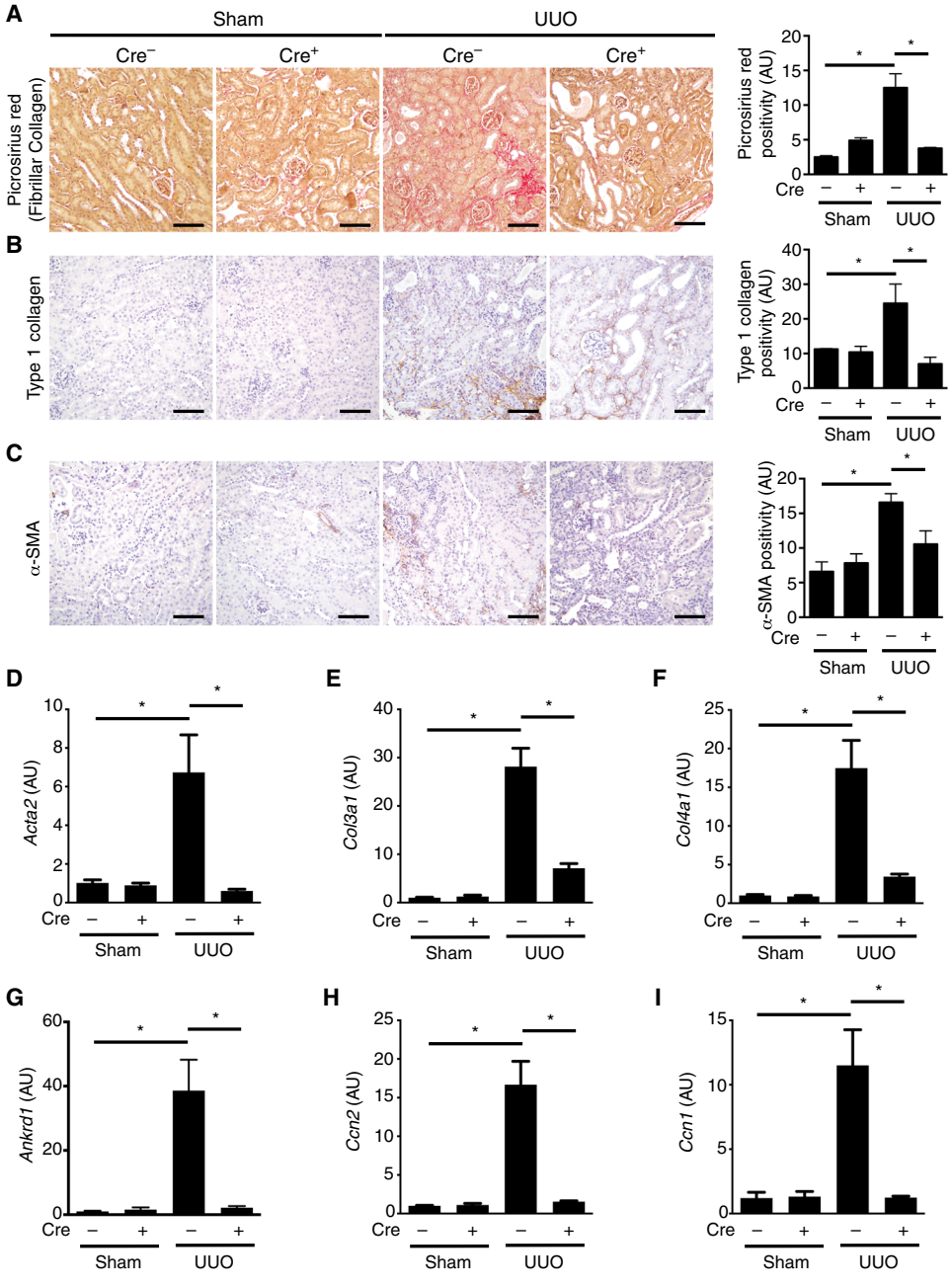

Fig. 5. Fibroblast-specific NUAK1 deficiency protects against kidney fibrosis. (**A** to **C**) Fibroblast-specific NUAK1-deficient mice (Col1a2-Cre/ERT$^{+/-}$ *Nuak1*$^{fl/fl}$) and their wild-type littermates (Col1a2-Cre/ERT$^{-/-}$ *Nuak1*$^{fl/fl}$) were randomized to sham surgery ($n = 3$ per group) or left-sided UUO ($n = 7$ Col1a2-Cre/ERT$^{-/-}$ *Nuak1*$^{fl/fl}$ and $n = 4$ Col1a2-Cre/ERT$^{+/-}$ *Nuak1*$^{fl/fl}$). Tamoxifen was administered between days 0 and 6 after surgery to activate expressed Cre recombinase. Left kidneys were harvested 7 days after surgery. Kidney sections were stained with (A) picrosirius red (PSR) to label fibrillar collagen, (B) an antibody directed against type 1 collagen, or (C) an antibody directed against α-SMA. Scale bars, 100 μm. RNA was also isolated from kidney homogenates and reverse-transcribed. The amounts of (**D**) *Acta2*, (**E**) *Col3a1*, (**F**) *Col4a1*, (**G**) *Ankrd1*, (**H**) *Ccn2*, and (**I**) *Ccn1* were determined using semiquantitative reverse transcription polymerase chain reaction. All transcript amounts were normalized to that of *Gapdh*. One-way ANOVA with post hoc Fisher's least significant difference was used for comparisons. Quantitative data are presented as means ± SEM. *$P < 0.05$.

Last, given that YAP is an important driver of fibrosis in multiple different tissues (*10*, *12*, *13*, *15*–*19*), we tested whether fibroblast NUAK1 deficiency would protect against fibrosis in other organs. Intratracheal bleomycin, a well-described profibrotic irritant (*42*, *43*), administered to wild-type mice induced lung fibrosis, whereas fibroblast-specific NUAK1-deficient littermates were protected against lung fibrosis (fig. S15). The reduction in fibrosis was associated with improved lung function, as demonstrated by higher peripheral blood oxygenation in fibroblast-specific NUAK1-deficient mice (fig. S15D). Similarly, fibroblast-specific NUAK1-deficient mice were also markedly protected against carbon tetrachloride–induced liver fibrosis (fig. S16). Together, these data suggest that NUAK1 signaling plays an important role in the regulation of organ fibrosis.

Pharmacologic NUAK inhibition attenuates organ fibrosis

To explore the possibility of NUAK inhibition as an antifibrotic therapeutic strategy, we next treated mice with the NUAK inhibitor HTH-02-006, beginning immediately after UUO. Consistent with our observations in fibroblast-specific NUAK1-deficient mice, early initiation of HTH-02-006 treatment attenuated the development of both histologic and molecular markers of kidney fibrosis (Fig. 6). Similarly, early HTH-02-006 treatment also reduced bleomycin-induced lung fibrosis and improved blood oxygenation (fig. S17). Because early HTH-02-006 treatment had such a notable protective effect, we next tested whether delayed initiation of HTH-02-006 treatment could also attenuate the progression of established kidney fibrosis. Mice were therefore subjected to sham or UUO surgery and then randomized to receive HTH-02-006 or vehicle beginning 7 days after surgery. At this time point, fibrosis has already developed (Fig. 6) (*8*), mimicking the more clinically relevant setting when patients with established chronic kidney disease typically present for treatment. Consistent with its antifibrotic protective effect, delayed initiation of HTH-02-006 treatment reduced histologic and molecular markers of kidney fibrosis (fig. S18).

DISCUSSION

Using cell, mouse, and human systems, we show that NUAK1, a member of the AMPK family of serine/threonine kinases, is a critical and previously unrecognized driver of organ fibrosis. Specifically, we demonstrate that after fibrotic injury, the amount of NUAK1 increases, driven by the key profibrotic

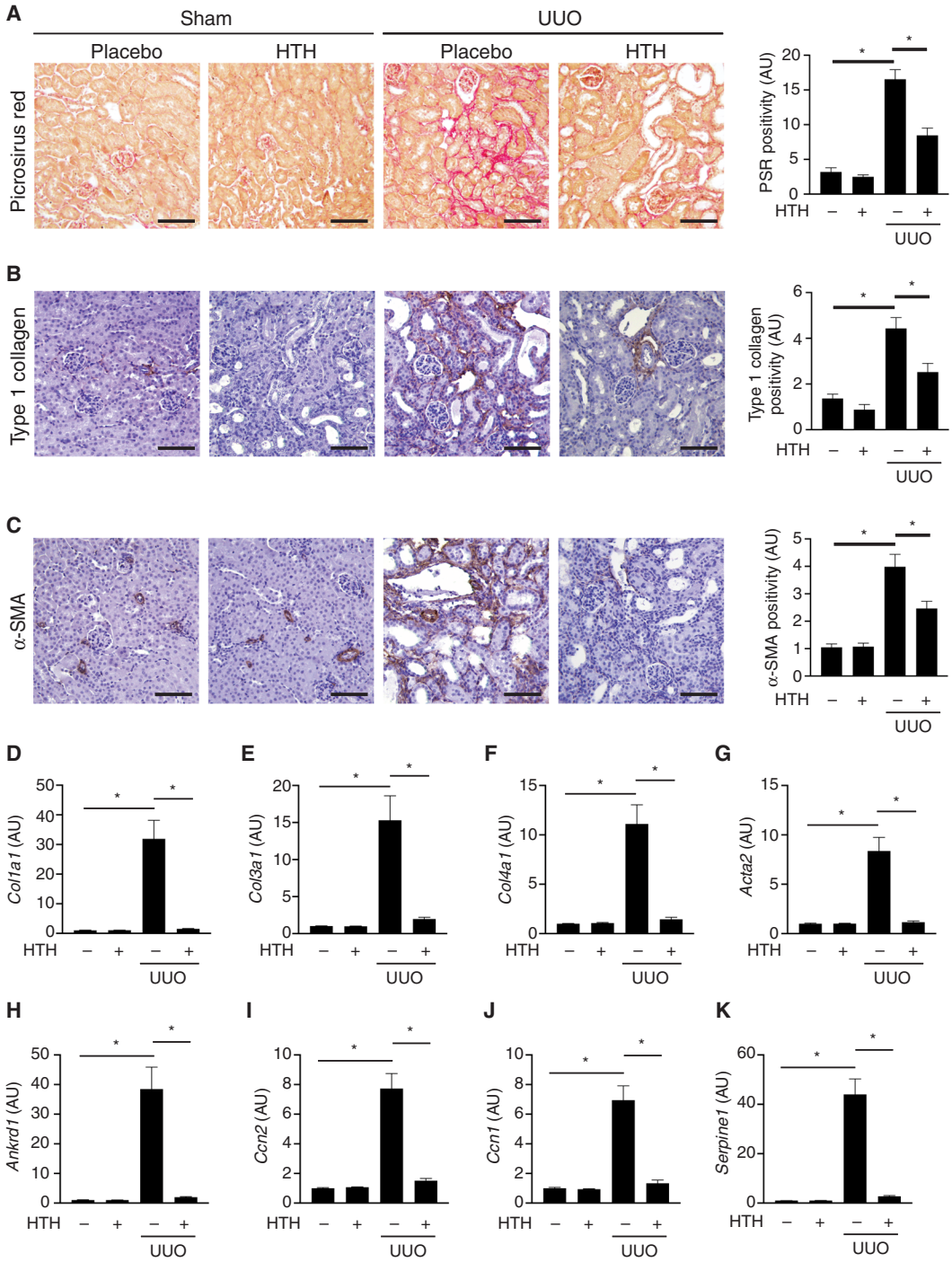

Fig. 6. Early treatment with the NUAK inhibitor HTH-02-006 attenuates UUO-induced renal fibrosis. Male C57BL/6 mice were subjected to sham surgery or left-sided UUO. Immediately after surgery, mice were randomized to receive twice daily intraperitoneal injections of either HTH-02-006 (10 mg/kg; $n = 6$ sham and $n = 16$ UUO) or DMSO vehicle ($n = 6$ sham and $n = 12$ UUO). Seven days after surgery, left kidneys were harvested, and sections were stained with (**A**) PSR to label fibrillar collagen, (**B**) an antibody directed against type 1 collagen, or (**C**) an antibody directed against α-SMA. Scale bars, 100 μm. The amounts of mRNA of (**D**) *Col1a1*, (**E**) *Col3a1*, (**F**) *Col4a1*, and (**G**) *Acta2*, as well as those of (**H**) *Ankrd1*, (**I**) *Ccn2*, (**J**) *Ccn1*, and (**K**) *Serpine1* were examined using quantitative polymerase chain reaction of cDNA prepared from whole-kidney homogenates. Transcript amounts were normalized to the housekeeper transcript *Gapdh*. One-way ANOVA with post hoc Fisher's least significant difference was used for comparisons. Quantitative data are presented as means ± SEM. *$P < 0.05$.

regulators TGF-β, YAP, and TAZ. We further show that NUAK1 facilitates profibrotic YAP and TGF-β/SMAD signaling. Together, our results suggest the existence of a TGF-β–inducible NUAK1-YAP/SMAD signaling loop that drives fibrogenesis. Because TGF-β/SMADs, YAP, and TAZ are not easily targetable, these data point to the exciting potential for NUAK1 inhibition as an antifibrotic treatment strategy that interrupts this critical fibrotic signaling loop.

Multiple lines of evidence from a variety of organs point to the important roles that YAP and TAZ play in promoting fibroblast activation (*10*, *12*, *13*, *15*–*18*). Despite their importance in the regulation of fibrosis, a critical unanswered question has been how YAP and TAZ are activated after injury. YAP and TAZ are regulated by a series of serine/threonine kinases that comprise the Hippo pathway (*44*–*46*). Multiple stimuli are known to control Hippo pathway kinase activity, including biochemical cues such as nutrient status (*47*–*50*) and G protein–coupled receptor signaling (*51*) and biomechanical signals such as ECM stiffness (*14*, *52*–*54*). Our data suggest that TGF-β–mediated induction of NUAK1 protein may be another possible mechanism of YAP activation, which, in turn, induces a fibrogenic gene program that ultimately leads to pathologic matrix production. Many of the genes induced in this fibrogenic program are co-regulated by both YAP and TGF-β/SMAD signaling (*33*). Thus, it is possible that TGF-β–induced increases in NUAK1 protein may also facilitate TGF-β/SMAD signaling, independent of its effects on YAP.

We also found that YAP (and TAZ) regulate *Nuak1* expression, because overexpression of constitutively active YAP and TAZ increased

Nuak1 mRNA and NUAK1 protein in NRK49F fibroblasts. Because these overexpression experiments likely induced supraphysiologic YAP and TAZ activation, we also silenced YAP and/or TAZ, finding that YAP and/or TAZ deficiency reduced *Nuak1* expression. In the context of our other findings, these results suggest the existence of a profibrotic positive feedback loop, whereby TGF-β–induced NUAK1 protein serves as an important node that facilitates both canonical TGF-β/SMAD signaling and noncanonical YAP signaling. YAP, in turn, induces additional NUAK1 expression, which can perpetuate this profibrotic signaling loop.

The only other published report that examined the role of NUAK1 in fibroblasts found that this enzyme inhibited TGF-β signaling in cultured skin fibroblasts (*29*). In contrast, our data, derived in kidney and lung fibroblasts, demonstrate that NUAK1 is a potent inducer of basal and TGF-β–induced fibrotic gene expression. We also demonstrate that fibroblast-specific deletion of *Nuak1* markedly attenuates fibrosis in vivo in two independent models of kidney disease and in models of lung and liver fibrosis. This apparently conflicting data suggest that NUAK1 may have different effects depending on cell type and local environment. Clearly, future studies are required to tease out the context-specific cues that control the effects of NUAK1.

Although we have demonstrated that NUAK1 can promote fibrosis possibly by YAP activation, the exact mechanisms underlying the YAP-regulating activity of NUAK1 need further examination. In the current study, we show that NUAK1 is required for TGF-β–induced dephosphorylation and nuclear localization of YAP, two key upstream YAP-activating events that, in most settings, are controlled by the Hippo pathway kinases large tumor suppressor kinase 1 (LATS1) and LATS2. The LATS kinases phosphorylate YAP on key serine residues, rendering YAP inactive by targeting it to the cytoplasm (*45*). Our results are thus in line with prior work showing that NUAKs can interact with LATS1 (*55*) and with our previous study showing that NUAK2, a close relative of NUAK1, inactivates LATS1 via phosphorylating two key residues (T246 and S613). However, our findings do not exclude other potential mechanisms of action for NUAK1, such as reports showing that NUAK2 can activate YAP by controlling cytoskeletal tension, a known YAP regulator, in a variety of epithelial and cancer cell lines (*38*).

YAP also promotes NUAK2 expression in cancer cells, leading to increased NUAK2 protein and thus further YAP activation (*38*, *56*). These data suggest that YAP works with NUAK2 in a positive feedback loop to drive cancer cell proliferation (*38*, *56*), in a manner similar to the profibrotic YAP-NUAK1 signaling loop that we describe in fibroblasts. Given these similarities, we examined the expression of both *NUAK1* and *NUAK2* in our cohort of human kidney biopsies. The amount of *NUAK1* mRNA, but not of *NUAK2*, correlated with fibrotic burden in these biopsies, suggesting that in the kidney, NUAK1 may play a more important role in fibrogenesis. Clearly, however, future studies will be required to more fully examine whether NUAK2 is involved in the pathogenesis of organ fibrosis. Regardless, because YAP and TAZ regulate many important cell processes, these findings raise the intriguing possibility that YAP/TAZ-NUAK positive feedback signaling may play an important role as an amplification mechanism for a variety of cellular functions.

In summary, we have identified NUAK1 as a profibrotic kinase that is up-regulated in multiple fibrotic mouse and human tissues, and which associates with poor outcomes in human chronic kidney disease, a condition that is driven by progressive fibrosis. Using a combination of cell and mouse studies, we define a potential mechanism by which NUAK1 promotes fibrosis. Our data suggest that TGF-β stimulates an increase in fibroblast NUAK1 that, in turn, promotes profibrotic YAP and SMAD signaling to induce the expression of a suite of fibrogenic genes. One of these genes is NUAK1, raising the possibility of a profibrotic NUAK1-YAP positive feedback loop. Our data therefore point to a previously unrecognized role for NUAK1 as an important promoter of progressive organ fibrosis. Unlike YAP, TAZ, and SMADs, NUAK1 is a kinase, raising the exciting possibility of traditional kinase inhibitor development as a means to target this critical profibrotic pathway.

MATERIALS AND METHODS

Study design

This study aimed to identify novel regulators of organ fibrosis. We first performed RNA-seq profiling of a convenience sample of archived human biopsy specimens, identifying NUAK1 as a kinase whose expression was strongly associated with fibrotic burden and renal outcomes. We next analyzed *Nuak1* expression in cell and murine models of fibrosis and explored its role in fibrosis regulation using genetic and pharmacologic tools to delete or inhibit *Nuak1*. The human kidney biopsy study cohort was a convenience sample, and thus, a formal sample size calculation was not performed. For in vitro and in vivo studies, sample sizes were calculated using a confidence interval of 95% and 80% power. Mice were randomly assigned to experimental groups. Outliers greater than 2 SDs from the mean were generally excluded. Histologic and molecular fibrosis end points standard for the field were selected for our mouse studies and analyzed by observers blinded to group assignment. Biological replicates for each experiment are included in the figure and table captions. Raw data for experiments are summarized in the appended data file S1.

Human kidney biopsy study

In this retrospective case control study, we analyzed a convenience sample of 18 archived human transplant kidney biopsies stored in the Department of Laboratory Medicine and Pathobiology at St. Michael's Hospital (*57*). The inclusion criteria were as follows: (i) Kidneys must have been transplanted >1 year prior, and (ii) sufficient tissue is needed to be available for RNA-seq. We also analyzed a convenience sample of the 12 most recently collected, archived kidney biopsies obtained from potential living kidney donors. These 12 biopsies contained no pathologic abnormalities and were thus used as healthy native kidney controls. This retrospective study was approved by the St. Michael's Hospital Research Ethics Board (REB 16-118). The requirement for written informed consent was waived because the study met the criteria for waiver of consent as outlined in the Tri-Council Policy Statement 2 Guidelines (Canada) and Personal Health Information Protection Act (Ontario). Details of data collection are provided in the Supplementary Materials.

RNA sequencing

RNA was extracted from kidney biopsy tissue, and complementary DNA (cDNA) libraries were prepared and sequenced on an Illumina HiSeq 2000 or 3000 (*57*), as described in the Supplementary Materials. RNA yield, read numbers per sample, and other relevant data are summarized in table S4. truRPM [transcript union reads per million (RPM) reads] values, which include reads mapped to both intron and exon reads, were calculated using in-house scripts and represent

overall transcript amount normalized by total mapped reads. An unrelated control sample was included in the processing pipeline to verify the integrity of the output. Data are deposited in Gene Expression Omnibus (GEO) (accession no. GSE135327).

Analytical pipelines

To determine correlations with clinical data, truRPM data for each transcript that passed low-expression filters (~13,500 genes) were then correlated with Banff histologic fibrosis score and slope of eGFR change after biopsy using Spearman's correlation analyses. The resulting individual Spearman's correlation coefficients were then plotted in two-dimensional matrices, and significance boundaries were determined by permutation testing. For this, the truRPMs of the transplant samples were randomly sampled within genes, and the Spearman correlations with the slope of eGFR change and the Banff histologic fibrosis score were recalculated for multiple rounds of 1000 iterations, and for multiple cutoff ranges, to calculate quadrant boundaries corresponding to $P = 0.02$, which revealed 290 genes significantly associated with outcome. These outcome-associated genes were manually curated and organized on heatmaps generated with ggplot2 (*58*). Next, a fibroblast–TGF-β–regulated gene signature, consisting of 54 genes, was derived from Bottinger and Ju (*28*). The full set of filtered RPM data for the transplant samples and this 54-gene signature were used in the Broad Institute's ssGSEA (v9.1.1) web application (*59*) on the GenePattern cloud server (cloud.genepattern.org) (*59*) to calculate individual normalized enrichment scores using the full gene signature for each of the 18 samples, which demonstrate the differential expression of the gene set in each sample. The ssGSEA cloud tool was run with the log sample normalization method and a weighting exponent value of 0.75. These normalized enrichment scores were then plotted against the expression of *NUAK1* in the samples using the *z* scores of the truRPMs.

Cell culture and treatments

Immortalized normal rat kidney interstitial fibroblasts (NRK49F, catalog no. CRL-1570) were purchased from American Type Culture Collection, and human lung fibroblasts from patients with idiopathic pulmonary fibrosis were purchased from Lonza (catalog no. CC-7231). Cells were cultured at 37°C with 5% CO_2 and grown in Dulbecco's modified Eagle's medium (DMEM) with 5% fetal bovine serum (FBS) or Fibroblast Growth Medium-2 (Lonza). After an overnight 16-hour serum deprivation (DMEM + 0.5% FBS), cells grown on gelatin-coated gels were stimulated with TGF-β (5 ng/ml; R&D Systems), 1 μM WZ4003 (Cayman Chemical), 100 nM HTH-02-006 (Ontario Institute for Cancer Research), 2.5 μM verteporfin (MilliporeSigma Canada), and/or 1 μM SB-431542 (Tocris Bioscience, Bio-Techne Canada) for the indicated times. For silencing experiments, NRK49F fibroblasts were transfected with siRNAs targeting *Nuak1*, *Yap*, *Taz*, *Smad2*, or *Smad3*. A scrambled siRNA was used as a negative control (see table S5 for siRNA sequences). siRNAs were transfected at a concentration of 10 nM using Lipofectamine RNAiMAX (Invitrogen). For overexpression experiments, NRK49F fibroblasts were transfected with plasmids encoding human YAP5SA, human TAZ4SA, human wild-type NUAK1 (gift of H. Zoghbi), or human kinase-deficient NUAK1 (K84M, Addgene) using Lipofectamine 2000 (Invitrogen) (*60*).

Immunoblotting

Cell lysates were separated by SDS–polyacrylamide gel electrophoresis, and after transfer, membranes were blotted with the following primary antibodies: YAP (1:1000 dilution; catalog nos. 14074 and 38707, Cell Signaling Technology), phospho-S127 YAP (1:1000 dilution; catalog no. 4911, Cell Signaling Technology), TAZ (1:1000 dilution; catalog no. 83669, Cell Signaling Technology), phospho-TAZ (S89) (1:500 dilution; catalog no. 59971, Cell Signaling Technology), NUAK1 (1:500 dilution; catalog no. 4458, Cell Signaling Technology), phospho-SMAD3 (1:1000 dilution; catalog no. 9520, Cell Signaling Technology), total SMAD3 (1:1000 dilution; catalog no. 9523, Cell Signaling Technology), and glyceraldehyde-3-phosphate dehydrogenase (GAPDH) (1:5000 dilution; catalog no. 2118, Cell Signaling Technology; catalog no. 9482, Abcam). Primary antibodies were detected with horseradish peroxidase–conjugated donkey anti-rabbit (1:10,000 dilution; catalog no. 711-035-152), donkey anti-mouse (1:10,000 dilution; catalog no. 715-035-150), and donkey anti-goat (1:10,000 dilution; catalog no. 705-035-003) secondary antibodies (Jackson ImmunoResearch). GAPDH protein amount was used for normalization. Quantitative analysis of band intensity was performed using ImageJ.

Terminal deoxynucleotidyl transferase–mediated deoxyuridine triphosphate nick end labeling

After fixation with 4% paraformaldehyde for 15 min at room temperature, cells were permeabilized with 0.1% Triton X-100 in phosphate-buffered saline (PBS) for 15 min at room temperature. Cells were then stained using a commercial terminal deoxynucleotidyl transferase–mediated deoxyuridine triphosphate nick end labeling (TUNEL) kit (catalog no. 11684795910, Sigma-Aldrich Canada) and 4′,6-diamidino-2-phenylindole for 1 hour at 37°C. Cells were washed with PBS and then mounted with Dako mounting media. Images were taken with a Zeiss LSM 700 confocal microscope (Carl Zeiss Canada), and pictures were analyzed and exported with Zeiss ZEN software (Carl Zeiss Canada). The percentage of $TUNEL^+$ cells was then calculated using a minimum of 45 cells per replicate.

Semiquantitative reverse transcription polymerase chain reaction

After various treatments as outlined in the text, RNA was collected from NRK49F fibroblasts and mouse kidney, lung, and liver tissues. The RNA was then reverse-transcribed, and the amounts of *Col1a1*, *Col3a1*, *Col4a1*, *Acta2*, *Ankrd1*, *Ccn2*, *Ccn1*, *Serpine1*, *Nuak1*, *Smad2*, *Smad3*, *Yap*, *Taz*, and/or *Gapdh* were quantified. Primer sequences are summarized in table S6. Experiments were performed in triplicate. Data analyses were performed using the Applied Biosystems Comparative CT method. All values were referenced to the amount of mRNA of the housekeeper gene *Gapdh*.

Luciferase reporter assay

NRK49F fibroblasts were transfected with a pGL3-Basic Firefly luciferase reporter (Promega) fused to 10 TEAD-binding sites (TGGAATGT) in tandem and a minimal Hsp70 promoter (*37*) and a pCMV5 vector encoding β-galactosidase. After 24 hours, cells were lysed in lysis buffer, and luciferase and β-galactosidase activity were measured using a Synergy Neo microplate reader (BioTek) and a SpectraMax M5e Multi-Mode plate reader (Molecular Devices) according to our previously published protocol (*56*).

Animal experiments

All animal studies were approved by the St. Michael's Hospital Animal Ethics Committee and conformed to the Canadian Council

on Animal Care guidelines. Wild-type C57BL/6 mice were purchased from Charles River Laboratories. In some experiments, mice were treated intraperitoneally with a NUAK inhibitor HTH-02-006 (10 mg/kg; synthesized by the Ontario Institute for Cancer Research) dissolved in 10% dimethyl sulfoxide (DMSO) or DMSO vehicle control twice daily. In other experiments, using a proα2(I) collagen promoter–driven tamoxifen-inducible Cre recombinase expression system, mice with either fibroblast-specific YAP/TAZ deficiency (Col1a2-Cre/ERT$^{+/-}$ and *Yap*$^{fl/fl}$, *Taz*$^{fl/fl}$ mice) or fibroblast-specific NUAK1 deficiency (Col1a2-Cre/ERT$^{+/-}$ and *Nuak1*$^{fl/fl}$ mice) on a mixed background were used. Mice were kept on a 12-hour light-dark cycle with ad libitum access to food and water. Mice were subjected to various fibrosis injury models in controlled laboratory experiments, including UUO, folic acid nephropathy, bleomycin-induced lung fibrosis, and carbon tetrachloride–induced liver fibrosis. All outcomes were assessed by a blinded observer. Further details of the animal experiments are included in the Supplementary Materials.

Tissue collection, preparation, and histochemistry

At study end, the kidneys, lungs, and/or livers of mice were harvested, and samples of each tissue were immersion-fixed in 10% neutral buffered formalin, embedded in cryostat matrix (Tissue-Tek, VWR), and/or stored in RNAlater (Invitrogen).

Immunofluorescence staining

NRK49F fibroblasts cultured on gelatin-coated gels and formalin-fixed paraffin-embedded kidney sections were immunostained and imaged using an LSM 700 inverted laser scanning confocal microscope (Carl Zeiss Canada) (*61*, *62*). Kidney sections were also stained with an RNAscope probe targeting *Nuak1* mRNA (catalog no. 434281, Advanced Cell Diagnostics). Details are provided in the Supplementary Materials.

Histochemistry, immunohistochemistry, and in situ hybridization

Formalin-fixed tissues were embedded in paraffin and sectioned before staining with picrosirius red (Sigma-Aldrich), hematoxylin and eosin, Masson's trichrome, or antibodies against α-SMA (1:100 dilution; catalog no. M085129-2, Dako) and type I collagen (1:200 dilution; catalog no. 1310-01, Southern Biotechnology) (*8*, *63*–*65*). Sections were also subjected to in situ hybridization with RNAscope. Full details are provided in Supplementary Materials. A minimum of four random, nonoverlapping 20× images of kidney cortex, liver, and/or lung were taken by a blinded observer using an upright Olympus light microscope and then analyzed in a blinded fashion using Aperio Imagescope software (Leica Biosystems) as previously described (*8*, *63*–*65*). Lung injury was measured using semiquantitative Ashcroft scoring as previously described (*66*).

Hydroxyproline content measurement

Hydroxyproline content was measured using a commercial assay kit (catalog no. K226, BioVision), following a slightly modified version of the manufacturer's protocol as described in the Supplementary Materials (*67*).

Statistical analysis

A minimum of three independent experiments was performed for all in vitro studies. Data presented are means ± SEM, unless otherwise indicated. For all in vitro and mouse studies, between-group differences were measured using two-tailed Student's *t* test (α = 95%) or one-way analysis of variance (ANOVA) with Fisher's least significant difference post hoc analysis where appropriate. Spearman's correlation analysis and univariate linear regression were also performed. Statistical analysis was performed using GraphPad Prism for Mac 6.0 (GraphPad Software) and R (version 3.4.3, R Foundation for Statistical Computing). Statistical analysis of the human kidney biopsy RNA-seq data is described above.

SUPPLEMENTARY MATERIALS

www.science.org/doi/10.1126/scitranslmed.aaz4028
Materials and Methods
Figs. S1 to S18
Tables S1 to S6
Data file S1
MDAR Reproducibility Checklist

View/request a protocol for this paper from *Bio-protocol*.

REFERENCES AND NOTES

1. T. A. Wynn, Common and unique mechanisms regulate fibrosis in various fibroproliferative diseases. *J. Clin. Invest.* **117**, 524–529 (2007).
2. D. C. Rockey, P. D. Bell, J. A. Hill, Fibrosis—A common pathway to organ injury and failure. *N. Engl. J. Med.* **372**, 1138–1149 (2015).
3. M. Nangaku, Chronic hypoxia and tubulointerstitial injury: A final common pathway to end-stage renal failure. *J. Am. Soc. Nephrol.* **17**, 17–25 (2006).
4. L. G. Fine, J. T. Norman, Chronic hypoxia as a mechanism of progression of chronic kidney diseases: From hypothesis to novel therapeutics. *Kidney Int.* **74**, 867–872 (2008).
5. W. A. Border, N. A. Noble, Transforming growth factor beta in tissue fibrosis. *N. Engl. J. Med.* **331**, 1286–1292 (1994).
6. W. A. Border, E. Ruoslahti, Transforming growth factor-beta in disease: The dark side of tissue repair. *J. Clin. Invest.* **90**, 1–7 (1992).
7. A. Leask, D. J. Abraham, TGF-β signaling and the fibrotic response. *FASEB J.* **18**, 816–827 (2004).
8. S. G. Szeto, M. Narimatsu, M. Lu, X. He, A. M. Sidiqi, M. F. Tolosa, L. Chan, K. De Freitas, J. F. Bialik, S. Majumder, S. Boo, B. Hinz, Q. Dan, A. Advani, R. John, J. L. Wrana, A. Kapus, D. A. Yuen, YAP/TAZ are mechanoregulators of TGF-β-smad signaling and renal fibrogenesis. *J. Am. Soc. Nephrol.* **27**, 3117–3128 (2016).
9. B. Piersma, S. de Rond, P. M. Werker, S. Boo, B. Hinz, M. M. van Beuge, R. A. Bank, YAP1 is a driver of myofibroblast differentiation in normal and diseased fibroblasts. *Am. J. Pathol.* **185**, 3326–3337 (2015).
10. M. Liang, M. Yu, R. Xia, K. Song, J. Wang, J. Luo, G. Chen, J. Cheng, Yap/taz deletion in Gli(+) cell-derived myofibroblasts attenuates fibrosis. *J. Am. Soc. Nephrol.* **28**, 3278–3290 (2017).
11. A. Futakuchi, T. Inoue, F. Y. Wei, M. Inoue-Mochita, T. Fujimoto, K. Tomizawa, H. Tanihara, YAP/TAZ are essential for TGF-β2–mediated conjunctival fibrosis. *Invest. Ophthalmol. Vis. Sci.* **59**, 3069–3078 (2018).
12. F. Liu, D. Lagares, K. M. Choi, L. Stopfer, A. Marinkovic, V. Vrbanac, C. K. Probst, S. E. Hiemer, T. H. Sisson, J. C. Horowitz, I. O. Rosas, L. E. Fredenburgh, C. Feghali-Bostwick, X. Varelas, A. M. Tager, D. J. Tschumperlin, Mechanosignaling through YAP and TAZ drives fibroblast activation and fibrosis. *Am. J. Physiol. Lung Cell. Mol. Physiol.* **308**, L344–L357 (2015).
13. I. Mannaerts, S. B. Leite, S. Verhulst, S. Claerhout, N. Eysackers, L. F. Thoen, A. Hoorens, H. Reynaert, G. Halder, L. A. van Grunsven, The Hippo pathway effector YAP controls mouse hepatic stellate cell activation. *J. Hepatol.* **63**, 679–688 (2015).
14. S. Dupont, L. Morsut, M. Aragona, E. Enzo, S. Giulitti, M. Cordenonsi, F. Zanconato, J. Le Digabel, M. Forcato, S. Bicciato, N. Elvassore, S. Piccolo, Role of YAP/TAZ in mechanotransduction. *Nature* **474**, 179–183 (2011).
15. X. Varelas, R. Sakuma, P. Samavarchi-Tehrani, R. Peerani, B. M. Rao, J. Dembowy, M. B. Yaffe, P. W. Zandstra, J. L. Wrana, TAZ controls Smad nucleocytoplasmic shuttling and regulates human embryonic stem-cell self-renewal. *Nat. Cell Biol.* **10**, 837–848 (2008).
16. X. Varelas, P. Samavarchi-Tehrani, M. Narimatsu, A. Weiss, K. Cockburn, B. G. Larsen, J. Rossant, J. L. Wrana, The Crumbs complex couples cell density sensing to Hippo-dependent control of the TGF-β-SMAD pathway. *Dev. Cell* **19**, 831–844 (2010).
17. P. Speight, M. Kofler, K. Szaszi, A. Kapus, Context-dependent switch in chemo/mechanotransduction via multilevel crosstalk among cytoskeleton-regulated MRTF and TAZ and TGFβ-regulated Smad3. *Nat. Commun.* **7**, 11642 (2016).
18. S. Noguchi, A. Saito, Y. Mikami, H. Urushiyama, M. Horie, H. Matsuzaki, H. Takeshima, K. Makita, N. Miyashita, A. Mitani, T. Jo, Y. Yamauchi, Y. Terasaki, T. Nagase, TAZ contributes to pulmonary fibrosis by activating profibrotic functions of lung fibroblasts. *Sci. Rep.* **7**, 42595 (2017).

19. S. Anorga, J. M. Overstreet, L. L. Falke, J. Tang, R. G. Goldschmeding, P. J. Higgins, R. Samarakoon, Deregulation of Hippo-TAZ pathway during renal injury confers a fibrotic maladaptive phenotype. *FASEB J.* **32**, 2644–2657 (2018).
20. A. Loupy, M. Haas, K. Solez, L. Racusen, D. Glotz, D. Seron, B. J. Nankivell, R. B. Colvin, M. Afrouzian, E. Akalin, N. Alachkar, S. Bagnasco, J. U. Becker, L. Cornell, C. Drachenberg, D. Dragun, H. de Kort, I. W. Gibson, E. S. Kraus, C. Lefaucheur, C. Legendre, H. Liapis, T. Muthukumar, V. Nickeleit, B. Orandi, W. Park, M. Rabant, P. Randhawa, E. F. Reed, C. Roufosse, S. V. Seshan, B. Sis, H. K. Singh, C. Schinstock, A. Tambur, A. Zeevi, M. Mengel, The banff 2015 kidney meeting report: Current challenges in rejection classification and prospects for adopting molecular pathology. *Am. J. Transplant.* **17**, 28–41 (2017).
21. L. Juillerat-Jeanneret, P. Tafelmeyer, D. Golshayan, Fibroblast activation protein-α in fibrogenic disorders and cancer: More than a prolyl-specific peptidase? *Expert Opin. Ther. Targets* **21**, 977–991 (2017).
22. H. Zhao, H. Bian, X. Bu, S. Zhang, P. Zhang, J. Yu, X. Lai, D. Li, C. Zhu, L. Yao, J. Su, Targeting of Discoidin Domain Receptor 2 (DDR2) prevents myofibroblast activation and neovessel formation during pulmonary fibrosis. *Mol. Ther.* **24**, 1734–1744 (2016).
23. H. Bian, X. Nie, X. Bu, F. Tian, L. Yao, J. Chen, J. Su, The pronounced high expression of discoidin domain receptor 2 in human interstitial lung diseases. *ERJ Open Res.* **4**, 00138–02016 (2018).
24. J. Andrae, R. Gallini, C. Betsholtz, Role of platelet-derived growth factors in physiology and medicine. *Genes Dev.* **22**, 1276–1312 (2008).
25. M. Teraishi, M. Takaishi, K. Nakajima, M. Ikeda, Y. Higashi, S. Shimoda, Y. Asada, A. Hijikata, O. Ohara, Y. Hiraki, S. Mizuno, T. Fukada, T. Furukawa, N. Wakamatsu, S. Sano, Critical involvement of ZEB2 in collagen fibrillogenesis: The molecular similarity between Mowat-Wilson syndrome and Ehlers-Danlos syndrome. *Sci. Rep.* **7**, 46565 (2017).
26. D. F. Higgins, K. Kimura, W. M. Bernhardt, N. Shrimanker, Y. Akai, B. Hohenstein, Y. Saito, R. S. Johnson, M. Kretzler, C. D. Cohen, K. U. Eckardt, M. Iwano, V. H. Haase, Hypoxia promotes fibrogenesis in vivo via HIF-1 stimulation of epithelial-to-mesenchymal transition. *J. Clin. Invest.* **117**, 3810–3820 (2007).
27. N. Ferrari, R. Ranftl, I. Chicherova, N. D. Slaven, E. Moeendarbary, A. J. Farrugia, M. Lam, M. Semiannikova, M. C. W. Westergaard, J. Tchou, L. Magnani, F. Calvo, Dickkopf-3 links HSF1 and YAP/TAZ signalling to control aggressive behaviours in cancer-associated fibroblasts. *Nat. Commun.* **10**, 130 (2019).
28. E. P. Bottinger, W. Ju, in *Smad Signal Transduction: Proteins and Cell Regulation*, P. Dijke, C. H. Heldin, Eds. (Springer, 2006), pp. 335–360.
29. C. Kolliopoulos, E. Raja, M. Razmara, P. Heldin, C. H. Heldin, A. Moustakas, L. P. van der Heide, Transforming growth factor β (TGFβ) induces NUAK kinase expression to fine-tune its signaling output. *J. Biol. Chem.* **294**, 4119–4136 (2019).
30. F. Zanconato, M. Forcato, G. Battilana, L. Azzolin, E. Quaranta, B. Bodega, A. Rosato, S. Bicciato, M. Cordenonsi, S. Piccolo, Genome-wide association between YAP/TAZ/TEAD and AP-1 at enhancers drives oncogenic growth. *Nat. Cell Biol.* **17**, 1218–1227 (2015).
31. B. Zheng, Z. Zhang, C. M. Black, B. de Crombrugghe, C. P. Denton, Ligand-dependent genetic recombination in fibroblasts: A potentially powerful technique for investigating gene function in fibrosis. *Am. J. Pathol.* **160**, 1609–1617 (2002).
32. A. Reginensi, R. P. Scott, A. Gregorieff, M. Bagherie-Lachidan, C. Chung, D. S. Lim, T. Pawson, J. Wrana, H. McNeill, Yap- and Cdc42-dependent nephrogenesis and morphogenesis during mouse kidney development. *PLOS Genet.* **9**, e1003380 (2013).
33. T. A. Beyer, A. Weiss, Y. Khomchuk, K. Huang, A. A. Ogunjimi, X. Varelas, J. L. Wrana, Switch enhancers interpret TGF-β and hippo signaling to control cell fate in human embryonic stem cells. *Cell Rep.* **5**, 1611–1624 (2013).
34. H. Kanai, T. Tanaka, Y. Aihara, S. Takeda, M. Kawabata, K. Miyazono, R. Nagai, M. Kurabayashi, Transforming growth factor-beta/Smads signaling induces transcription of the cell type-restricted ankyrin repeat protein CARP gene through CAGA motif in vascular smooth muscle cells. *Circ. Res.* **88**, 30–36 (2001).
35. S. K. Leivonen, L. Hakkinen, D. Liu, V. M. Kahari, Smad3 and extracellular signal-regulated kinase 1/2 coordinately mediate transforming growth factor-beta-induced expression of connective tissue growth factor in human fibroblasts. *J. Invest. Dermatol.* **124**, 1162–1169 (2005).
36. L. Bartholin, L. L. Wessner, J. M. Chirgwin, T. A. Guise, The human Cyr61 gene is a transcriptional target of transforming growth factor beta in cancer cells. *Cancer Lett.* **246**, 230–236 (2007).
37. A. L. Couzens, J. D. Knight, M. J. Kean, G. Teo, A. Weiss, W. H. Dunham, Z. Y. Lin, R. D. Bagshaw, F. Sicheri, T. Pawson, J. L. Wrana, H. Choi, A.-C. Gingras, Protein interaction network of the mammalian Hippo pathway reveals mechanisms of kinase-phosphatase interactions. *Sci. Signal.* **6**, rs15 (2013).
38. W. C. Yuan, B. Pepe-Mooney, G. G. Galli, M. T. Dill, H. T. Huang, M. Hao, Y. Wang, H. Liang, R. A. Calogero, F. D. Camargo, NUAK2 is a critical YAP target in liver cancer. *Nat. Commun.* **9**, 4834 (2018).
39. S. Banerjee, S. J. Buhrlage, H. T. Huang, X. Deng, W. Zhou, J. Wang, R. Traynor, A. R. Prescott, D. R. Alessi, N. S. Gray, Characterization of WZ4003 and HTH-01-015 as selective inhibitors of the LKB1-tumour-suppressor-activated NUAK kinases. *Biochem. J.* **457**, 215–225 (2014).
40. M. Z. Miranda, J. F. Bialik, P. Speight, Q. Dan, T. Yeung, K. Szaszi, S. F. Pedersen, A. Kapus, TGF-β1 regulates the expression and transcriptional activity of TAZ protein via a Smad3-independent, myocardin-related transcription factor-mediated mechanism. *J. Biol. Chem.* **292**, 14902–14920 (2017).
41. A. A. Eddy, J. M. Lopez-Guisa, D. M. Okamura, I. Yamaguchi, Investigating mechanisms of chronic kidney disease in mouse models. *Pediatr. Nephrol.* **27**, 1233–1247 (2012).
42. N. C. Henderson, T. D. Arnold, Y. Katamura, M. M. Giacomini, J. D. Rodriguez, J. H. McCarty, A. Pellicoro, E. Raschperger, C. Betsholtz, P. G. Ruminski, D. W. Griggs, M. J. Prinsen, J. J. Maher, J. P. Iredale, A. Lacy-Hulbert, R. H. Adams, D. Sheppard, Targeting of αv integrin identifies a core molecular pathway that regulates fibrosis in several organs. *Nat. Med.* **19**, 1617–1624 (2013).
43. R. Kramann, R. K. Schneider, D. P. DiRocco, F. Machado, S. Fleig, P. A. Bondzie, J. M. Henderson, B. L. Ebert, B. D. Humphreys, Perivascular Gli1+ progenitors are key contributors to injury-induced organ fibrosis. *Cell Stem Cell* **16**, 51–66 (2015).
44. G. Halder, R. L. Johnson, Hippo signaling: Growth control and beyond. *Development* **138**, 9–22 (2011).
45. B. Zhao, X. Wei, W. Li, R. S. Udan, Q. Yang, J. Kim, J. Xie, T. Ikenoue, J. Yu, L. Li, P. Zheng, K. Ye, A. Chinnaiyan, G. Halder, Z. C. Lai, K. L. Guan, Inactivation of YAP oncoprotein by the Hippo pathway is involved in cell contact inhibition and tissue growth control. *Genes Dev.* **21**, 2747–2761 (2007).
46. S. Wu, J. Huang, J. Dong, D. Pan, hippo encodes a Ste-20 family protein kinase that restricts cell proliferation and promotes apoptosis in conjunction with salvador and warts. *Cell* **114**, 445–456 (2003).
47. W. Wang, Z. D. Xiao, X. Li, K. E. Aziz, B. Gan, R. L. Johnson, J. Chen, AMPK modulates Hippo pathway activity to regulate energy homeostasis. *Nat. Cell Biol.* **17**, 490–499 (2015).
48. J. S. Mo, Z. Meng, Y. C. Kim, H. W. Park, C. G. Hansen, S. Kim, D. S. Lim, K. L. Guan, Cellular energy stress induces AMPK-mediated regulation of YAP and the Hippo pathway. *Nat. Cell Biol.* **17**, 500–510 (2015).
49. M. DeRan, J. Yang, C. H. Shen, E. C. Peters, J. Fitamant, P. Chan, M. Hsieh, S. Zhu, J. M. Asara, B. Zheng, N. Bardeesy, J. Liu, X. Wu, Energy stress regulates hippo-YAP signaling involving AMPK-mediated regulation of angiomotin-like 1 protein. *Cell Rep.* **9**, 495–503 (2014).
50. E. Enzo, G. Santinon, A. Pocaterra, M. Aragona, S. Bresolin, M. Forcato, D. Grifoni, A. Pession, F. Zanconato, G. Guzzo, S. Bicciato, S. Dupont, Aerobic glycolysis tunes YAP/TAZ transcriptional activity. *EMBO J.* **34**, 1349–1370 (2015).
51. F. X. Yu, B. Zhao, N. Panupinthu, J. L. Jewell, I. Lian, L. H. Wang, J. Zhao, H. Yuan, K. Tumaneng, H. Li, X. D. Fu, G. B. Mills, K. L. Guan, Regulation of the Hippo-YAP pathway by G-protein-coupled receptor signaling. *Cell* **150**, 780–791 (2012).
52. M. Aragona, T. Panciera, A. Manfrin, S. Giulitti, F. Michielin, N. Elvassore, S. Dupont, S. Piccolo, A mechanical checkpoint controls multicellular growth through YAP/TAZ regulation by actin-processing factors. *Cell* **154**, 1047–1059 (2013).
53. L. Sansores-Garcia, W. Bossuyt, K. Wada, S. Yonemura, C. Tao, H. Sasaki, G. Halder, Modulating F-actin organization induces organ growth by affecting the Hippo pathway. *EMBO J.* **30**, 2325–2335 (2011).
54. K. Wada, K. Itoga, T. Okano, S. Yonemura, H. Sasaki, Hippo pathway regulation by cell morphology and stress fibers. *Development* **138**, 3907–3914 (2011).
55. N. Humbert, N. Navaratnam, A. Augert, M. Da Costa, S. Martien, J. Wang, D. Martinez, C. Abbadie, D. Carling, Y. de Launoit, J. Gil, D. Bernard, Regulation of ploidy and senescence by the AMPK-related kinase NUAK1. *EMBO J.* **29**, 376–386 (2010).
56. M. K. Gill, T. Christova, Y. Y. Zhang, A. Gregorieff, L. Zhang, M. Narimatsu, S. Song, S. Xiong, A. L. Couzens, J. Tong, J. R. Krieger, M. F. Moran, A. R. Zlotta, T. H. van der Kwast, A. C. Gingras, F. Sicheri, J. L. Wrana, L. Attisano, A feed forward loop enforces YAP/TAZ signaling during tumorigenesis. *Nat. Commun.* **9**, 3510 (2018).
57. X. He, M. F. Tolosa, T. Zhang, S. K. Goru, L. U. Severino, P. S. Misra, C. M. McEvoy, L. Caldwell, S. G. Szeto, F. Gao, X. Chen, C. Atin, V. Ki, N. Vukosa, C. Hu, J. Zhang, C. Yip, A. Krizova, J. L. Wrana, D. A. Yuen, Myofibroblast YAP/TAZ activation is a key step in organ fibrogenesis. *JCI Insight.* **7**, e146243 (2022).
58. H. Wickham, ggplot2: Elegant Graphics for Data Analysis (Springer-Verlag, 2016).
59. D. A. Barbie, P. Tamayo, J. S. Boehm, S. Y. Kim, S. E. Moody, I. F. Dunn, A. C. Schinzel, P. Sandy, E. Meylan, C. Scholl, S. Frohling, E. M. Chan, M. L. Sos, K. Michel, C. Mermel, S. J. Silver, B. A. Weir, J. H. Reiling, Q. Sheng, P. B. Gupta, R. C. Wadlow, H. Le, S. Hoersch, B. S. Wittner, S. Ramaswamy, D. M. Livingston, D. M. Sabatini, M. Meyerson, R. K. Thomas, E. S. Lander, J. P. Mesirov, D. E. Root, D. G. Gilliland, T. Jacks, W. C. Hahn, Systematic RNA interference reveals that oncogenic KRAS-driven cancers require TBK1. *Nature* **462**, 108–112 (2009).
60. C. A. Lasagna-Reeves, M. de Haro, S. Hao, J. Park, M. W. Rousseaux, I. Al-Ramahi, P. Jafar-Nejad, L. Vilanova-Velez, L. See, A. De Maio, L. Nitschke, Z. Wu, J. C. Troncoso, T. F. Westbrook, J. Tang, J. Botas, H. Y. Zoghbi, Reduction of Nuak1 decreases tau and reverses phenotypes in a tauopathy mouse model. *Neuron* **92**, 407–418 (2016).
61. S. Chaturvedi, D. A. Yuen, A. Bajwa, Y. W. Huang, C. Sokollik, L. Huang, G. Y. Lam, S. Tole, G. Y. Liu, J. Pan, L. Chan, Y. Sokolskyy, M. Puthia, G. Godaly, R. John, C. Wang, W. L. Lee,

J. H. Brumell, M. D. Okusa, L. A. Robinson, Slit2 prevents neutrophil recruitment and renal ischemia-reperfusion injury. *J. Am. Soc. Nephrol.* **24**, 1274–1287 (2013).
62. S. Tole, I. M. Mukovozov, Y. W. Huang, M. A. Magalhaes, M. Yan, M. R. Crow, G. Y. Liu, C. X. Sun, Y. Durocher, M. Glogauer, L. A. Robinson, The axonal repellent, Slit2, inhibits directional migration of circulating neutrophils. *J. Leukoc. Biol.* **86**, 1403–1415 (2009).
63. D. A. Yuen, K. A. Connelly, A. Advani, C. Liao, M. A. Kuliszewski, J. Trogadis, K. Thai, S. L. Advani, Y. Zhang, D. J. Kelly, H. Leong-Poi, A. Keating, P. A. Marsden, D. J. Stewart, R. E. Gilbert, Culture-modified bone marrow cells attenuate cardiac and renal injury in a chronic kidney disease rat model via a novel antifibrotic mechanism. *PLOS ONE* **5**, e9543 (2010).
64. D. A. Yuen, K. A. Connelly, Y. Zhang, S. L. Advani, K. Thai, G. Kabir, D. Kepecs, C. Spring, C. Smith, I. Batruch, H. Kosanam, A. Advani, E. Diamandis, P. A. Marsden, R. E. Gilbert, Early outgrowth cells release soluble endocrine antifibrotic factors that reduce progressive organ fibrosis. *Stem Cells* **31**, 2408–2419 (2013).
65. Y. Zhang, D. A. Yuen, A. Advani, K. Thai, S. L. Advani, D. Kepecs, M. G. Kabir, K. A. Connelly, R. E. Gilbert, Early-outgrowth bone marrow cells attenuate renal injury and dysfunction via an antioxidant effect in a mouse model of type 2 diabetes. *Diabetes* **61**, 2114–2125 (2012).
66. T. Ashcroft, J. M. Simpson, V. Timbrell, Simple method of estimating severity of pulmonary fibrosis on a numerical scale. *J. Clin. Pathol.* **41**, 467–470 (1988).
67. A. J. Haak, E. Kostallari, D. Sicard, G. Ligresti, K. M. Choi, N. Caporarello, D. L. Jones, Q. Tan, J. Meridew, A. M. Diaz Espinosa, A. Aravamudhan, J. L. Maiers, R. D. Britt Jr., A. C. Roden, C. M. Pabelick, Y. S. Prakash, S. M. Nouraie, X. Li, Y. Zhang, D. J. Kass, D. Lagares, A. M. Tager, X. Varelas, V. H. Shah, D. J. Tschumperlin, Selective YAP/TAZ inhibition in fibroblasts via dopamine receptor D1 agonism reverses fibrosis. *Sci. Transl. Med.* **11**, (2019).

Acknowledgments: We wish to thank research staff N. Dacouris, L. Rapi, W. Yuan, D. Fogelman, and M. Nash for assistance in ethics board approvals, patient recruitment, data collection, and study coordination. We also wish to thank R. Prasad and J. Zaltzman for facilitating patient recruitment from their busy transplant clinics and A. Common, D. Marcuzzi, and V. Prabhudesai for performing all kidney biopsies. **Funding:** This work was supported by a Transitional Operating Grant (201503MOP-341962 to D.A.Y.) and a Project Scheme Grant (153039) from the Canadian Institutes of Health Research (CIHR; to D.A.Y.), as well as a Collaborative Health Research Project Grant cofunded by CIHR and the National Sciences and Engineering Research Council of Canada (to A. Kirpalani and D.A.Y.), funds from the St. Michael's Hospital Foundation (to D.A.Y.), and CIHR Foundation Grants (to L.A. and J.L.W.). S.K.G. and L.U.S. were supported by postdoctoral fellowships from the Banting and Best Diabetes Centre. S.K.G. was also supported by a KRESCENT postdoctoral fellowship. M.F.T. was supported by a Li Ka Shing Knowledge Scholarship. P.S.M. was supported by a KRESCENT postdoctoral fellowship. J.L.W. is the Mary Janigan Research Chair in Molecular Cancer Therapeutics. D.A.Y. was supported by a KRESCENT New Investigator and Canadian Diabetes Association Clinician Scientist salary support award and is a recipient of a CIHR New Investigator Award. **Author contributions:** T.Z. designed and performed experiments, conducted data analysis, and revised the manuscript. X.H., S.K.G., L.U.S., and T.C. designed and performed experiments and revised the manuscript. Y.L. prepared and tested HTH-02-006. L.C., P.S.M., and C.M.M. conducted bioinformatics analysis and revised the manuscript. M.F.T., C.A., J.Z., C.H., N.V., and X.C. conducted data analysis. A. Krizova reviewed biopsy histology. A. Kirpalani designed experiments and obtained funding. A.G. generated the *Nuak1*-floxed mice and reviewed the manuscript. R.N. and K.C. performed RNA-seq. M.K.G. designed and performed experiments and analyzed data. L.A. and J.L.W. designed experiments, analyzed data, obtained funding, and revised the manuscript. D.A.Y. designed experiments, analyzed data, obtained funding, and wrote and revised the manuscript. **Competing interests:** D.A.Y. and J.L.W. are scientific cofounders of, and consultants for, Fibrocor Therapeutics. The other authors declare that they have no competing interests. **Data and materials availability:** All data associated with this study are present in the paper or the Supplementary Materials. The RNA-seq data are deposited in GEO (accession no. GSE135327). A Flag-tagged wild-type human NUAK1 plasmid is available from H. Zoghbi under a material transfer agreement with the Baylor College of Medicine. Similarly, a Flag-tagged kinase-dead (K84M) human NUAK1 plasmid is available from Addgene under a material transfer agreement. The transgenic mice produced for this study (fibroblast-specific YAP/TAZ-deficient and fibroblast-specific NUAK1-deficient mice) or their precursors are available upon request.

Submitted 19 September 2019
Accepted 25 February 2022
Published 23 March 2022
10.1126/scitranslmed.aaz4028

Science Translational Medicine

NUAK1 promotes organ fibrosis via YAP and TGF-#/SMAD signaling

Tianzhou Zhang, Xiaolin He, Lauren Caldwell, Santosh Kumar Goru, Luisa Ulloa Severino, Monica F. Tolosa, Paraish S. Misra, Caitrona M. McEvoy, Tania Christova, Yong Liu, Cassandra Atin, Johnny Zhang, Catherine Hu, Noah Vukosa, Xiaolan Chen, Adriana Krizova, Anish Kirpalani, Alex Gregorieff, Ruoyu Ni, Kin Chan, Mandeep K. Gill, Liliana Attisano, Jeffrey L. Wrana, and Darren A. Yuen

Sci. Transl. Med., **14** (637), eaaz4028.
DOI: 10.1126/scitranslmed.aaz4028

Figuring out fibrogenesis

Transforming growth factor–# (TGF-#) drives fibrosis in part through YAP and TAZ transcription factors, but the link between tissue injury and transcription factor activation is unclear. Here, Zhang *et al.* discovered that the gene *NUAK1* was up-regulated in fibrotic human kidney tissue and mouse models of kidney, liver, and lung fibrosis. NUAK1 expression was regulated by TGF-#, YAP, and TAZ. Mice lacking *Nuak1* in fibroblasts were protected from fibrosis, and treatment with a NUAK1 inhibitor also attenuated fibrosis. The authors demonstrate that NUAK1 is induced by TGF-# and promotes YAP and TGF-#/SMAD signaling to drive fibrogenesis, supporting NUAK1 as a potential therapeutic target.

Science Translational Medicine (ISSN) is published by the American Association for the Advancement of Science. 1200 New York Avenue NW, Washington, DC 20005. The title *Science Translational Medicine* is a registered trademark of AAAS.